Supplementary Figure 1. Generation of mARD1A^{225} transgenic mice and Apc$^{Min/+}$ /mARD1A^{225} transgenic mice. **A)** Construction of mARD1A^{225} expression vectors. mARD1A^{225} cDNA was fused with the His9-HRV2-Myc9 tag. Gene expression was driven under the control of a chicken beta-actin promoter. **B)** Effects of mARD1A^{225} -9His-9Myc fusion protein on stability and acetylation of HIF-1α were confirmed in 293T cells using acetylation assays and visualized by Western blot with anti-HIF-1α antibody (1:1000). 293T cells were transfected with pCAGGS- mARD1A^{225} -9His-9Myc or mock vector (pCAGGS -9His-9Myc) and treated with proteasome inhibitor 10 uM MG132 under hypoxia for 4 hours (4H + MG132) **C)** Genotyping of mARD1A^{225} transgenic (Tg) mice by polymerase chain reaction (PCR) (**upper panel**) and Southern blot (**lower panel**). **D**) Expression levels of mARD1A^{225} -9His-9Myc protein determined in major organs of mARD1A^{225} Tg mice by Western blot analysis. **E)** Genotyping of Apc$^{Min/+}$ /mARD1A^{225} Tg mice mice by PCR. CBA promoter = chicken beta-actin promoter, IP = Immunoprecipitation, WB = Western blot analysis, GAPDH = Glyceraldehyde 3-phosphate dehydrogenase, nTg = non transgenic mouse.

Supplementary Figure 1

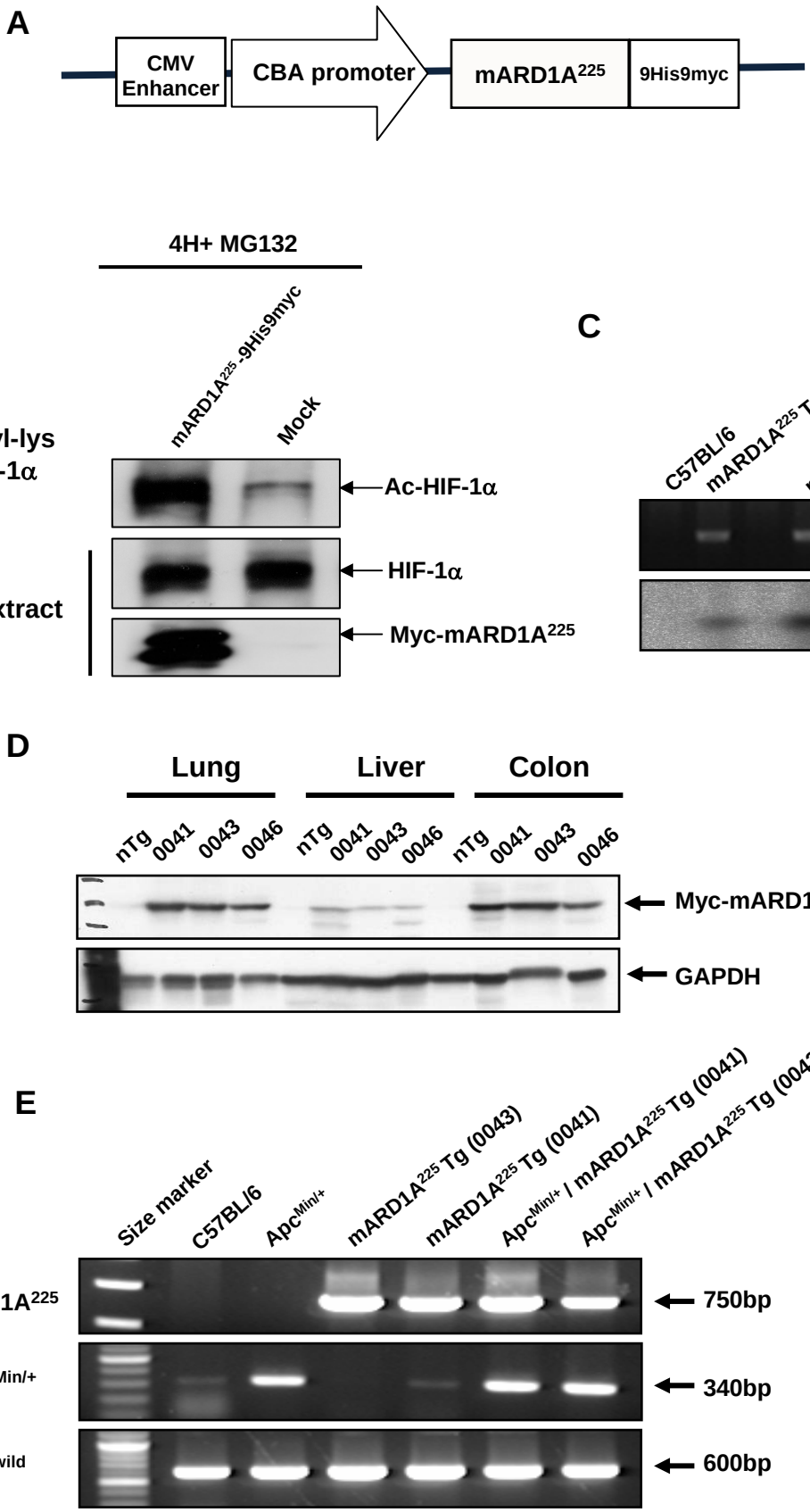

Supplementary Figure 2. Effect of transgenic overexpression of mARD1A^{225} on intestinal tumorigenesis in the transgenic line 0043. Number and size distribution of polyps in small intestines from Apc$^{Min/+}$(n=21 per group) and Apc$^{Min/+}$ /mARD1A^{225} Tg (n=8 per group, line 0043) mice. Polyps were classified according to size in millimeters. Results are means and 95% confidence intervals (CIs) (error bars). **P* = .04, ***P* = .03, compared with Apc$^{Min/+}$ mice, determined with the two-sided Mann-Whitney U test. (Apc$^{Min/+}$ mice vs Apc$^{Min/+}$ /mARD1A^{225} Tg mice, mean, all polyp sizes = 83.4 polyps vs 60.6 polyps, difference = 22.8 polyps, 95% CI = 34.7 to 49.3, *P* = .03; mean, large (>2mm) polyps = 23.1 polyps vs 8.8 polyps, difference = 14.3 polyps, 95% CI = 10 to 18.6, *P* = .04; mean medium (1-2mm) polyps = 52.3 polyps vs 41.7 polyps, difference = 10.6 polyps, 95% CI = 4.4 to16.8, *P* = .082; mean, small (<1mm) polyps = 7.9 polyps vs 10.1 polyps, difference = 2.2 polyps, 95% CI = 1.6 to 2.8, *P* = .081)

Supplementary Figure 2

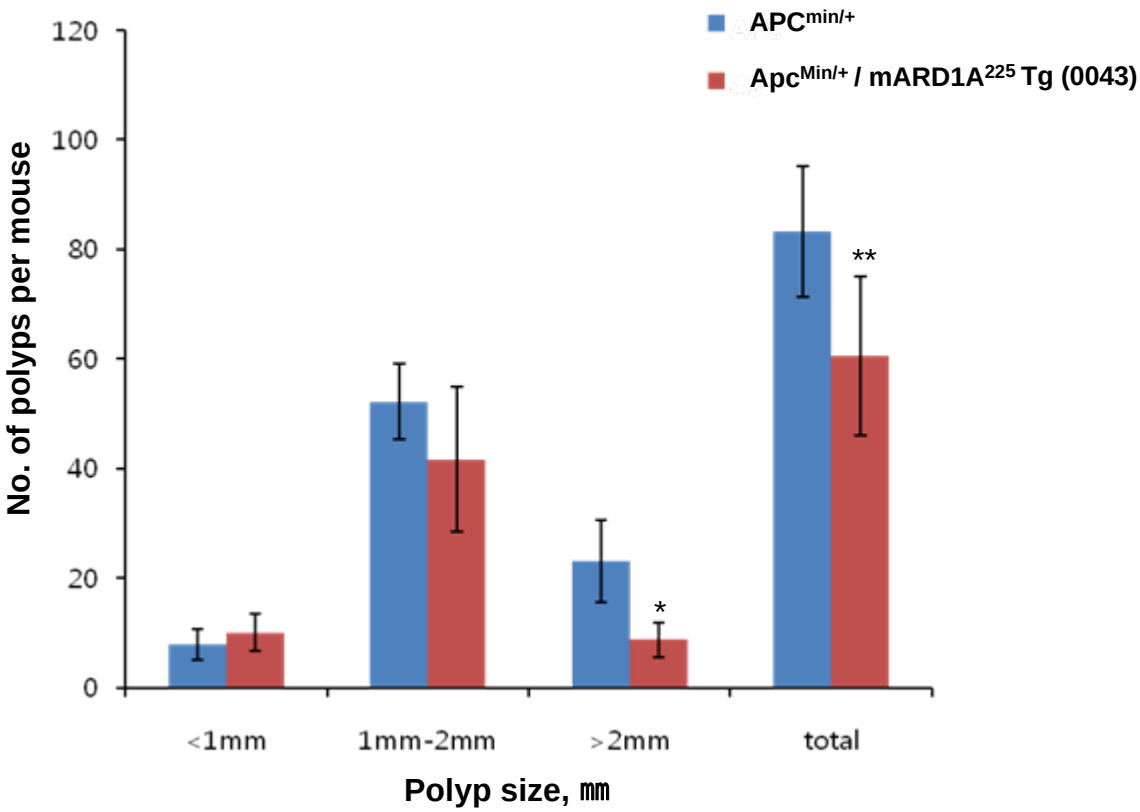

Supplementary Figure 3. Characterization of mARD1A^{225}-overexpressing tumor cells. **A)** B16F10, B16F1, MKN74, and NUGC-3 cell lines stably transfected with Myc-mARD1A^{225} were subjected to Western blot analysis with anti-Myc and anti-actin antibodies. **B)** Growth curves of mARD1A^{225}-transfected B16F10 (**left panel**) and MKN74 (**right panel**) cancer cells, B16F10-mock cells (**closed diamond**), two B16F10-mARD1A^{225} clones (**open triangle, square**), MKN74-mock cells (**closed diamond**) and two MKN74-mARD1A^{225} clones (**open triangle and square**). Three independent experiments were performed, each in three replicates. Results are means and 95% CIs (error bars) that derive from the means of the individual experiments (n=3). **C**) Cell diameters were determined by FACS analysis. SSC-H = side scatter; FSC-H = forward scatter. **D)** Phase-contrast micrographs of control and mARD1A^{225}-expressing tumor cells. Magnification, ×200. Scale bar = 50 ㎛. A#1 = B16F10-mARD1A^{225}#1; A#2 = B16F10-mARD1A^{225}#2; A#3 = MKN74-mARD1A^{225}#3; A#4 = MKN74-mARD1A^{225}#4; A#5 = B16F1-mARD1A^{225}#5; A#6 = B16F1-mARD1A^{225}#6; Ard = NUGC-3-mARD1A^{225}; A-Mix = before select a single clone.

Supplementary Figure 3

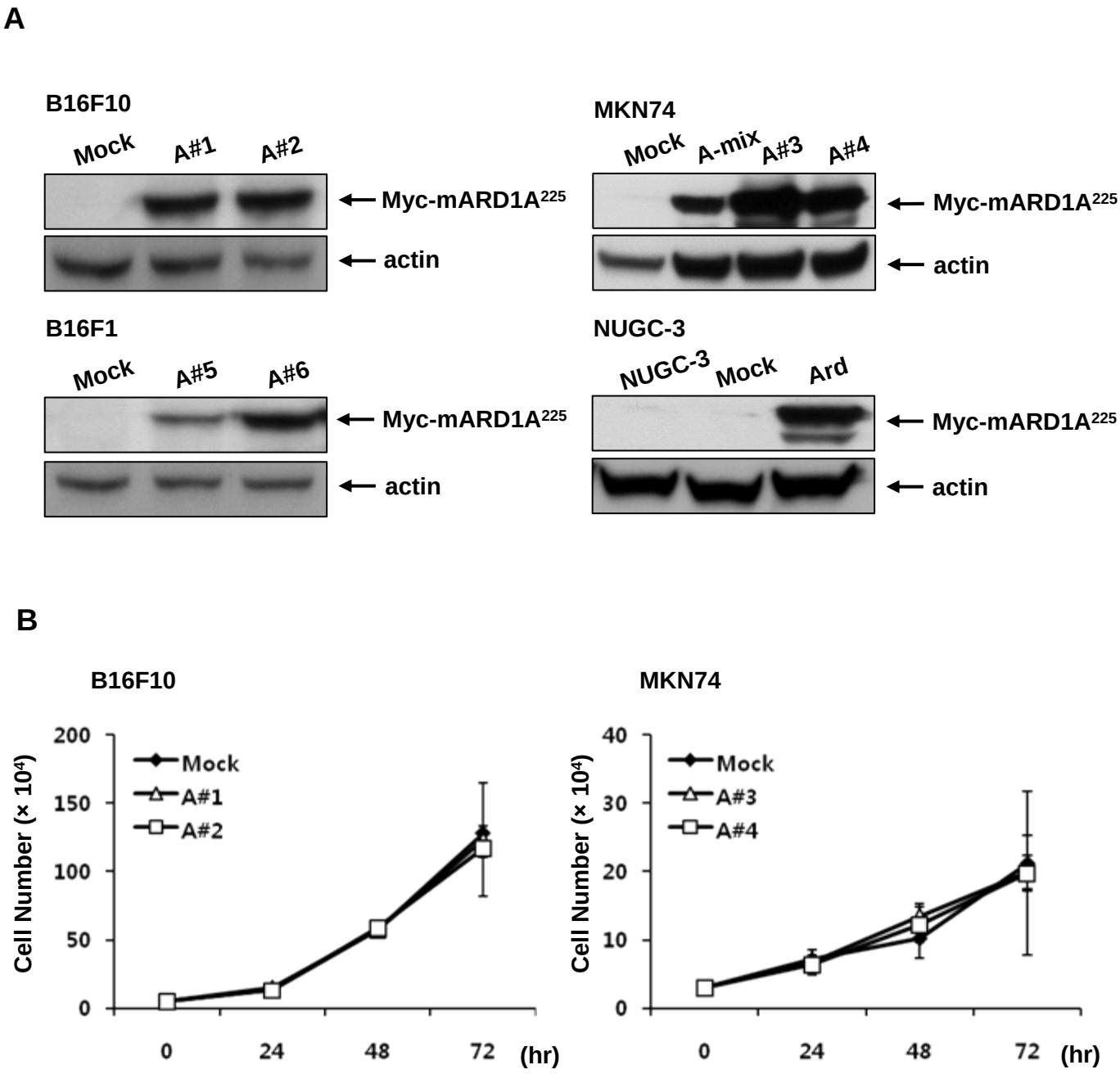

Supplementary Figure 3

C

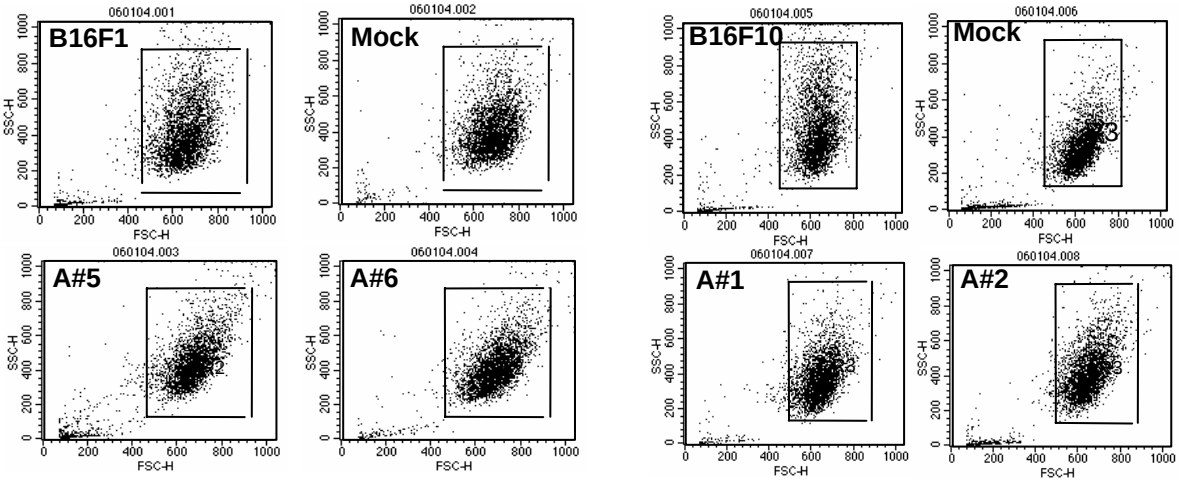

D

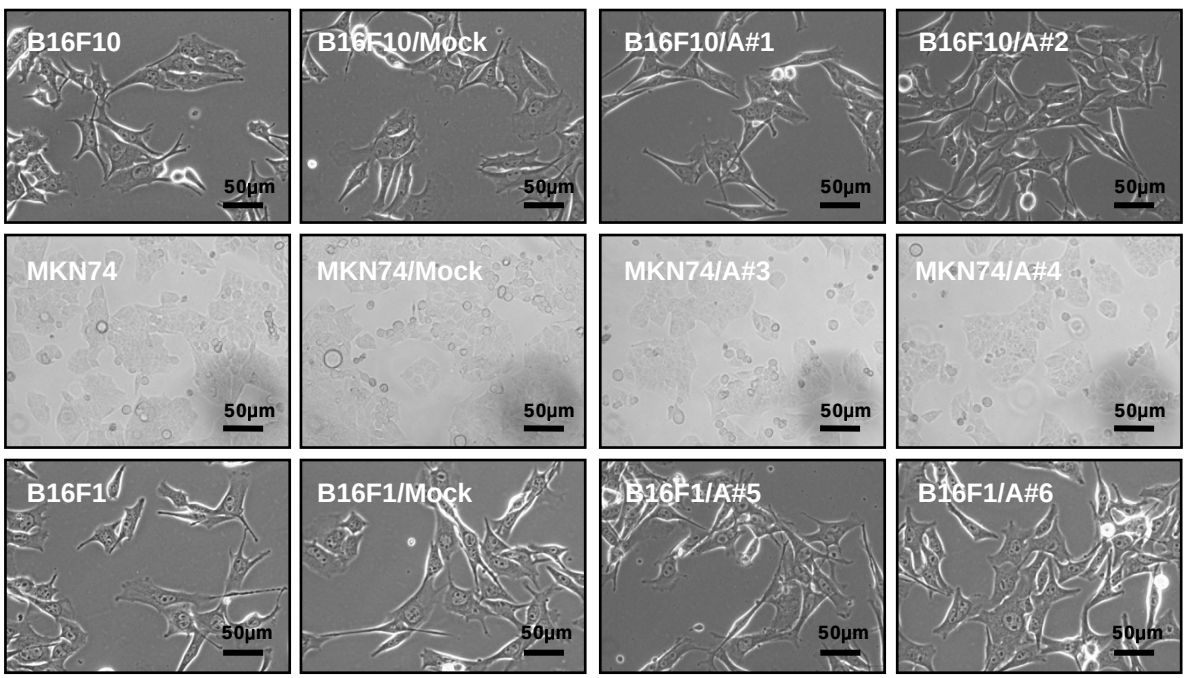

Supplementary Figure 4. Effect of mARD1A^{225} on growth of NUGC-3 human tumor cells in nude mice. Nude mice were injected subcutaneously with NUCG-3-mock (**open circle**) and NUGC-3- mARD1A^{225} cells (**closed square**), and monitored for tumor growth (n=5). Results are means and 95% CIs (error bars). At day 24, tumor volumes were as follows: NUCG-3-mock, mean = 36.4 mm^2, 95% CI = 75.4 to 148.2; NUGC-3- mARD1A^{225}, mean = 0 mm^2, 95% CI = 0 to 0.

Supplementary Figure 4

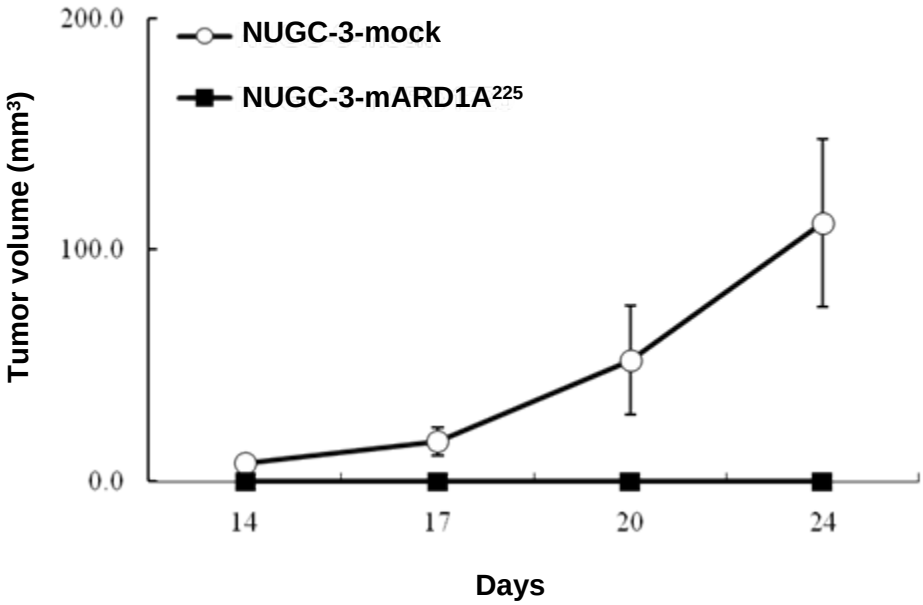

Supplementary Figure 5. Effects of mARD1A^{225} on expression and acetylation of HIF-1α. **A)** B16F1-mock and B16F1-mARD1A^{225} cells were exposed to 1% O_2 for 16 hours (16H). HIF-1 α protein levels were determined by Western blot analysis. **B)** NUGC-3-mock and NUGC-3-mARD1A^{225}cells were exposed to 1% O_2 (4H) or 21% O_2 (N) for 4 hours. HIF-1α and mARD1A^{225}protein levels were examined by Western blot analysis. The anti-Myc antibody was applied to detect m ARD1A^{225}. **C)** B16F1, B16F1-mock, and B16F1-mARD1A^{225} cells were exposed to 10 μM MG132 and 1% O_2 for 16 hours (16H+MG132). Cell lysates were immunoprecipitated with an anti-acetyl-lys antibody. Lysates and immunoprecipitates were subjected to Western blot analysis with an anti-HIF-1α antibody. A#5 = B16F1-mARD1A^{225}#5; A#6 = B16F1-mARD1A^{225}#6; Ard = NUGC-3-mARD1A^{225}.

Supplementary Figure 5

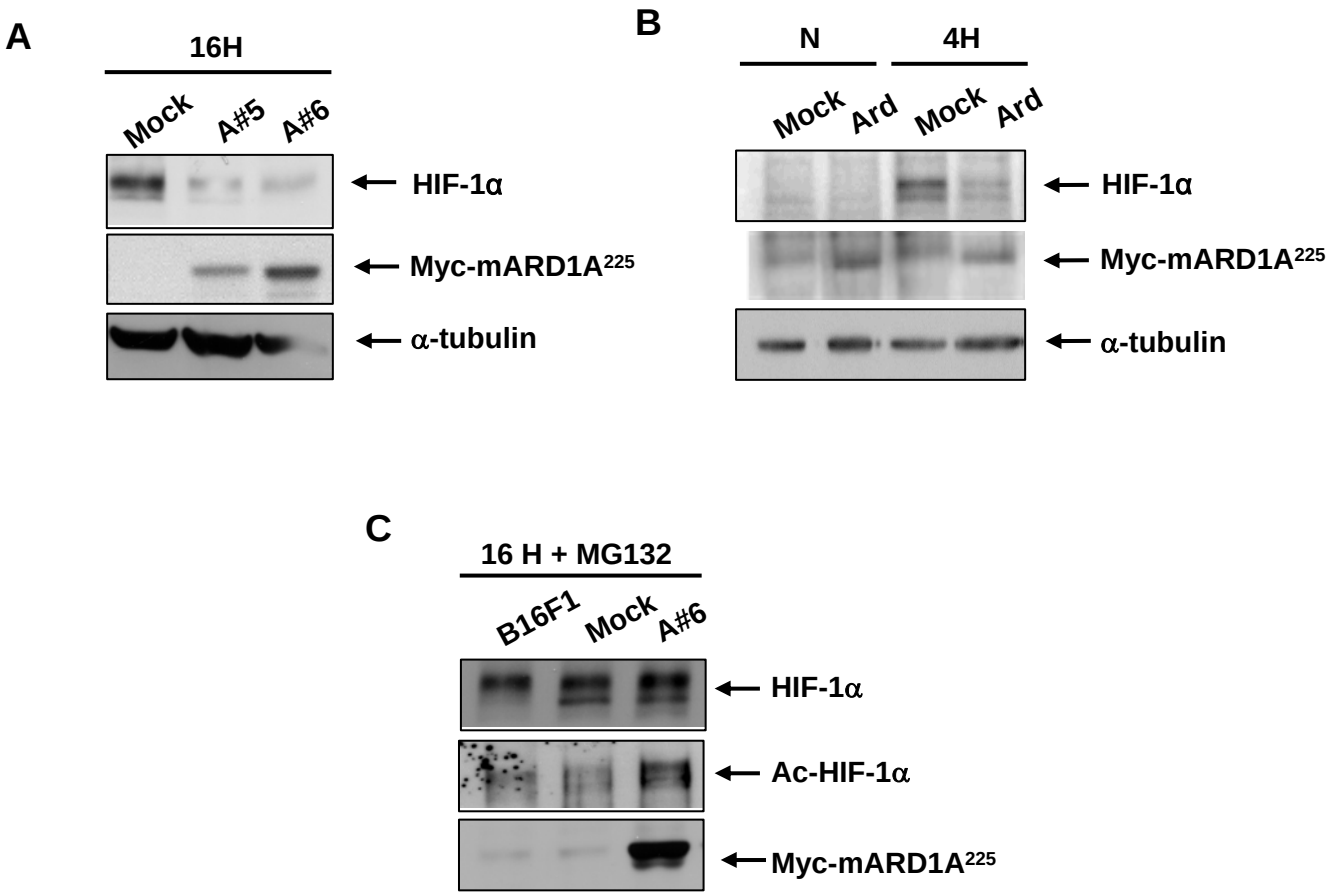

Supplementary Figure 6. Effect of mutant HIF-1α K532R on HIF-1α stabilization, cell migration, and lung nodule formation. **A)** B16F10-mock cells transfected with HIF-1α K532R were cultured under normoxic conditions. HIF-1α protein levels were determined by Western blot analysis. **B)** A linear injury line was created at the center of the cultured monolayer by scraping with a sterile pipette tip. Cells were incubated in the presence of 200 μM $CoCl_2$ for 24 hours. B16F10-mock-mock and B16F10-mock-HIF-1α K532R cells were treated with 3 μg/ml anti-mouse VEGFA antibody. Images of cell migration **(left panel)**. Quantification of cell migration (**right panel**). Three independent experiments were performed, each in two replicates. Results are means and 95% CIs (error bars) derived from the means of the individual experiments (n=3). Migration distance (μm): B16F10/mock-mock, mean = 360.4, 95% CI = 321.7 to 399; B16F10/mock-HIF-1α K532R, mean = 436.1, 95% CI = 406.5 to 465.7; B16F10/mock-mock + anti-VEGFA, mean = 157.1, 95% CI = 125.9 to 188.3; B16F10/mock-HIF-1α K532R + anti-VEGFA, mean = 127.2, 95% CI = 79 to 175.4; *P* values were determined using the two-sided Mann-Whitney U test. Magnification, × 100. Scale bar = 100 μm. **C)** C57BL/6 mice were injected intravenously with B16F10-mock-mock (n=15 mice) and B16F10-mock-HIF-1α K532R cells (n=15 mice). Lung nodule formation was determined 14 days after injection. Representative gross images of lungs (**left panel**). Number of surface tumor nodules (**right panel**). Results are means and 95% confidence intervals (CIs) (error bars). Number of lung nodules per mouse: B16F10/mock-mock, mean = 156.7 nodules, 95% CI = 121.5 to 191.9; B16F10/mock-HIF-1α K532R, mean = 247.6 nodules, 95% CI = 214.5 to 280.8; *P* value determined by two-sided Mann-Whitney U test. Mock/Mock = B16F10-mock-mock; Mock/HIF-1α K532R = B16F10-mock-HIF-1α K532R; Mock/Mock + anti-VEGFA = B16F10-mock-mock + anti-mouse VEGFA antibody; Mock/HIF-1α K532R + anti-VEGFA = B16F10-mock-HIF-1α K532R + anti-mouse VEGFA antibody.

Supplementary Figure 6